

Measurement of Spin–Lattice Relaxation Times and Concentrations in Systems with Chemical Exchange Using the One-Pulse Sequence: Breakdown of the Ernst Model for Partial Saturation in Nuclear Magnetic Resonance Spectroscopy

Richard G. S. Spencer and Kenneth W. Fishbein

National Institutes of Health, National Institute on Aging, GRC 4D-08, 5600 Nathan Shock Drive, Baltimore, Maryland 21224

Received May 7, 1999; accepted September 3, 1999

A fundamental problem in Fourier transform NMR spectroscopy is the calculation of observed resonance amplitudes for a repetitively pulsed sample, as first analyzed by Ernst and Anderson in 1966. Applications include determination of spin–lattice relaxation times (T_1 's) by progressive saturation and correction for partial saturation in order to determine the concentrations of the chemical constituents of a spectrum. Accordingly, the Ernst and Anderson formalism has been used in innumerable studies of chemical and, more recently, physiological systems. However, that formalism implicitly assumes that no chemical exchange occurs. Here, we present an analysis of N sites in an arbitrary chemical exchange network, explicitly focusing on the intermediate exchange rate regime in which the spin–lattice relaxation rates and the chemical exchange rates are comparable in magnitude. As a special case of particular importance, detailed results are provided for a system with three sites undergoing mutual exchange. Specific properties of the N -site network are then detailed. We find that (i) the Ernst and Anderson analysis describing the response of a system to repetitive pulsing is inapplicable to systems with chemical exchange and can result in large errors in T_1 and concentration measurements; (ii) T_1 's for systems with arbitrary exchange networks may still be correctly determined from a one-pulse experiment using the Ernst formula, provided that a short interpulse delay time and a large flip angle are used; (iii) chemical concentrations for exchanging systems may be correctly determined from a one-pulse experiment either by using a short interpulse delay time with a large flip angle, as for measuring T_1 's, and correcting for partial saturation by use of the Ernst formula, or directly by using a long interpulse delay time to avoid saturation; (iv) there is a significant signal-to-noise penalty for performing one-pulse experiments under conditions which permit accurate measurements of T_1 's and chemical concentrations. The present results are analogous to but are much more general than those that we have previously derived for systems with two exchanging sites. These considerations have implications for the design and interpretation of one-pulse experiments for all systems exhibiting chemical exchange in the intermediate exchange regime, including virtually all physiologic samples.

Key Words: chemical exchange; one-pulse experiment; saturation factors; partial saturation; progressive saturation.

INTRODUCTION

The simplest and still the most widely used NMR experiment is the one-pulse experiment, that is, the application of a long train of pulses of flip angle θ alternating with interpulse delays of duration TR, with signal acquisition after each pulse. This repetitively pulsed system rapidly and asymptotically approaches a cyclic steady state. The observed magnetization resulting from such an experiment was derived by Ernst and Anderson (1) when the use of Fourier transform NMR was becoming widespread. The Ernst and Anderson analysis is applicable to an isolated spin system and incorporates both longitudinal and transverse magnetization effects. The most commonly used form of their result, known as the Ernst equation, applies to the case in which $TR \gg T_2$, so that transverse magnetization effects may be neglected:

$$\frac{M_{\text{obs}}(\theta, TR)}{M_0} = \frac{(1 - e^{-TR/T_1}) \sin \theta}{(1 - e^{-TR/T_1} \cos \theta)}, \quad [1]$$

where M_0 is the equilibrium magnetization and $M_{\text{obs}}(\theta, TR)$ is the observed magnetization in the steady state resulting from a pulse sequence with parameters θ and TR.

It is evident from [1] that the spectral line will be of maximum amplitude, that is, $M_{\text{obs}}(\theta, TR) = M_0$, whenever $TR \rightarrow \infty$ and $\theta = 90^\circ$. Otherwise the saturation factor, SF, is defined as the ratio of the steady-state observed magnetization to the equilibrium magnetization and is a function of θ , TR, and T_1 for an isolated spin

$$\begin{aligned} \text{SF}(T_1; \theta, TR) &= \frac{M_{\text{obs}}(\theta, TR)}{M_0} \\ &= \frac{\text{resonance amplitude}(\theta, TR)}{\text{equilibrium resonance amplitude}}. \quad [2] \end{aligned}$$

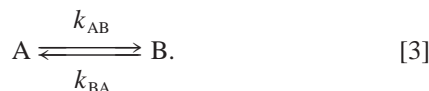
According to this formulation, the SF for each resonance in a

multicomponent spectrum is entirely independent of the presence or properties of other resonances.

Expressions [1] and [2] are used widely in NMR spectroscopy and imaging. One application is to the measurement of T_1 's by progressive saturation (2), in which SF's are observed for a series of values of TR for fixed θ . The resulting resonance amplitudes are then fit to Eq. [1] to obtain T_1 . Similarly, T_1 maps in magnetic resonance imaging are obtained by a pixel-by-pixel fit to an equation of this form.

In addition, as shown by Ernst and Anderson, large improvements in the signal-to-noise ratio (SNR) per unit time can be achieved by use of $TR \cong T_1$ and $\theta < 90^\circ$. The condition $TR \cong T_1$ results in resonance saturation, that is, inability of the magnetization vector to fully relax to M_0 by the end of the interpulse delay. The amplitude loss resulting from this can be corrected by measuring the resonance's T_1 and then determining the fully unsaturated resonance amplitude by use of Eq. [1]. More commonly, a correction based on Eq. [2] is implemented in which the SF is measured by comparing the amplitude of the resonance obtained with a long TR to the amplitude obtained with a shorter TR, for a fixed θ . This empirically measured SF is then used to correct subsequent amplitude measurements. Both of these approaches require that the SF depends only on the values of TR and θ for a given T_1 .

However, as we have shown in previous theoretical and experimental work (3–5), Eq. [1] is valid only in the case in which the species under consideration is not in chemical exchange. These papers treated the case of two species, A and B, undergoing exchange in the intermediate regime in which the spin–lattice relaxation rates and the chemical exchange rates are comparable in magnitude. The pseudo-unimolecular exchange rates k_{AB} and k_{BA} are defined by the reaction scheme



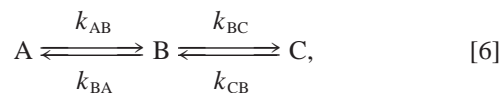
This problem was originally treated (3) by considering the solution to the relevant system of Bloch–McConnell equations (6) for two-site exchange and using this solution to derive the appropriate steady state. It was shown that the observed saturation factor for a resonance, e.g., A, depends not only on the flip angle and TR of the pulse sequence and T_{1A} , as is the case for nonexchanging species, but also on T_{1B} , k_{AB} , M_{0A} , and M_{0B} . Thus, Eq. [2] is replaced by

$$\frac{M_{\text{obs}}}{M_0} = \text{SF}(M_{0A}, M_{0B}, T_{1A}, T_{1B}, k_{AB}; \theta, \text{TR}), \quad [4]$$

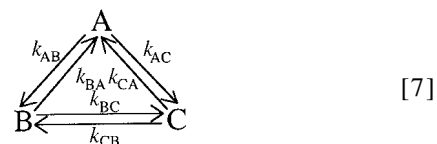
where the dependence on k_{BA} is implicit in the equation defining the chemical steady state:

$$k_{BA} = \frac{M_{0A}}{M_{0B}} k_{AB}. \quad [5]$$

However, in many chemical and physiologic systems exchange occurs among multiple sites. For example, three-site exchange networks can be of either the linear form,



or the cyclic form,



Systems with a greater number of exchanging compounds obviously may have more complex patterns.

For three-site exchange it is possible but difficult to carry through a calculation analogous to the original one (3) for two sites by solving the coupled Bloch–McConnell equations and then deriving the appropriate steady state. However, this explicit computation in closed form becomes completely intractable for four or more sites and provides little insight into the properties of the general N -site exchange network. Accordingly, we present here a formalism that permits us to easily address the three-site problem, can be readily generalized to include additional sites, and allows us to obtain general results for the N -site system.

The organization of the paper is as follows. The general theory is first presented, followed by detailed simulation results for the three-site case. After a description of the effect of exchange on saturation factors, the practical problem of accurate T_1 measurement is addressed. An apparent spin–lattice relaxation time, T_1' , which results from incorrectly ignoring chemical exchange in a T_1 measurement, is defined. The deviation of T_1' from the true T_1 is investigated as a function of pulse repetition time and flip angle, which are the only two parameters which can be readily varied by the investigator. Practical bounds are provided for TR and flip angle to achieve accurate measurements. The question of accurate concentration measurements as derived from magnetization measurements in a three-site exchanging system is then investigated. The deviation of apparent concentration ratios from true concentration ratios is investigated, and specific parameter constraints are provided which ensure accuracy. Finally, general properties of the N -site case are developed.

THEORY

Our physical picture of the development of the cyclic steady state will follow that of Ernst and Anderson (1), who consid-

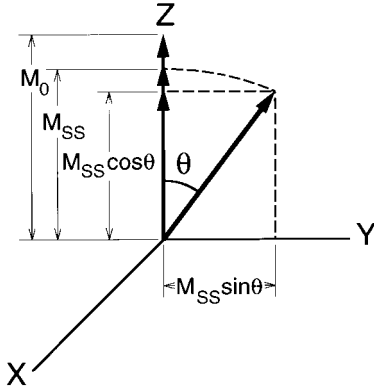


FIG. 1. Magnetization vector diagram showing the sequence of events that occurs in setting up the periodic steady state under repetitive pulsing. M_0 denotes the equilibrium magnetization of a species, M_{ss} denotes the steady-state value of the z -magnetization of that species, and θ is the pulse flip angle.

ered an isolated spin system subjected to a long sequence of alternating pulses and interpulse delays. Starting from a steady-state magnetization along the z -axis of amplitude M_{ss} , the spins are subjected to an \bar{x} -phase pulse of flip angle θ (see Fig. 1). Immediately after the pulse, the magnetization vector has components along both the z - and the y -axes. In this treatment, we are assuming that the time scale of T_2 processes is short, so that the magnetization vector immediately becomes oriented along the z -axis with amplitude $M_{ss} \cos \theta$. Starting from this initial condition, the vector then undergoes longitudinal relaxation over the time TR , reaching a value of M_{ss} at the time of the next pulse. It is clear that $M_{ss} = M_0$ only when $TR \gg T_1$. Note that the magnetization observed during this steady state, M_{obs} , is given by the transverse component immediately following the pulse, that is, $M_{ss} \sin \theta$.

More formally, during the interpulse delay of duration TR , the z -component of the magnetization evolves according to the Bloch equation

$$\frac{dM}{dt} = \frac{M_0 - M}{T_1} \quad [8]$$

with the solution

$$M(t) = M_0 - (M_0 - M(t=0))e^{-t/T_1}. \quad [9]$$

Once the steady state as defined above has been established, the relationships

$$M(t=0) = M_{ss} \cos \theta \quad [10]$$

and

$$M(TR) = M_{ss} \quad [11]$$

are satisfied. Then

$$M_{ss} = M_0 - (M_0 - M_{ss} \cos \theta) e^{-TR/T_1}, \quad [12]$$

from which one obtains

$$\frac{M_{ss}}{M_0} = \frac{1 - e^{-TR/T_1}}{1 - e^{-TR/T_1} \cos \theta}. \quad [13]$$

The observed magnetization following a pulse is therefore

$$M_{obs} = M_{ss} \sin \theta = M_0 \frac{(1 - e^{-TR/T_1}) \sin \theta}{1 - e^{-TR/T_1} \cos \theta}. \quad [14]$$

In the case of two species undergoing exchange, Eq. [8] must be replaced by the coupled system (6)

$$\frac{dM_A}{dt} = \frac{M_{0A} - M_A}{T_{1A}} - k_{AB}M_A + k_{BA}M_B \quad [15a]$$

$$\frac{dM_B}{dt} = \frac{M_{0B} - M_B}{T_{1B}} + k_{AB}M_A - k_{BA}M_B \quad [15b]$$

and the steady state constraint

$$k_{AB}M_{0A} = k_{BA}M_{0B}. \quad [16]$$

This was the system analyzed in detail in previous work (3–5). Corresponding experiments on an *in vitro* system with two-site exchange (4) and an *in vivo* system with three-site exchange (5) were also presented.

We now describe the analysis for a general N -site exchange network, composed of exchanging species S_i , $i \in (1, \dots, N)$, with pseudo-unimolecular rate constants $k_{S_i S_j}$ referring to the reaction from species S_i to species S_j .

The Bloch–McConnell equations describing the system are

$$\frac{dM_{S_i}}{dt} = \frac{M_{0S_i} - M_{S_i}}{T_{1S_i}} - \sum_{j \neq i} k_{S_i S_j} M_{S_i} + \sum_{j \neq i} k_{S_j S_i} M_{S_j}, \quad [17]$$

which may be conveniently written in matrix form as

$$\frac{d\mathbf{M}}{dt} = \mathbf{A}\mathbf{M} + \mathbf{C}, \quad [18]$$

where

$$\mathbf{M} = (M_{S_1}, M_{S_2}, \dots, M_{S_N}), \quad [19]$$

$$\mathbf{A} = \begin{pmatrix} -\left(\frac{1}{T_{1S_1}} + \sum_{j \neq 1} k_{S_1S_j}\right) & k_{S_2S_1} & \cdots & k_{S_NS_1} \\ k_{S_1S_2} & -\left(\frac{1}{T_{1S_2}} + \sum_{j \neq 2} k_{S_2S_j}\right) & \cdots & k_{S_NS_2} \\ \cdots & \cdots & \cdots & \cdots \\ k_{S_1S_N} & k_{S_2S_N} & \cdots & -\left(\frac{1}{T_{1S_N}} + \sum_{j \neq N} k_{S_NS_j}\right) \end{pmatrix} \quad [20]$$

and

$$\mathbf{C} = \left(\frac{M_{0S_1}}{T_{1S_1}}, \frac{M_{0S_2}}{T_{1S_2}}, \dots, \frac{M_{0S_N}}{T_{1S_N}} \right). \quad [21]$$

Note that the vector components here and in the following refer to the chemical species under consideration and not to spatial dimensions. We are assuming rapid transverse relaxation, so that all magnetizations are directed along the z -axis.

The solution to this system of linear differential equations may be found readily to be

$$\mathbf{M}(t) = e^{\mathbf{A}t}(\mathbf{M}(t=0) + \mathbf{A}^{-1}\mathbf{C}) - \mathbf{A}^{-1}\mathbf{C}, \quad [22]$$

where $\mathbf{M}(t=0)$ is the initial condition. To calculate the steady-state magnetization we use the fact that

$$\mathbf{M}(t=0) = \mathbf{M}_{ss} \cos \theta \quad [23]$$

and

$$\mathbf{M}(\text{TR}) = \mathbf{M}_{ss} \quad [24]$$

in the cyclic steady state, where

$$\mathbf{M}_{ss} = (M_{ssS_1}, M_{ssS_2}, \dots, M_{ssS_N}). \quad [25]$$

Then

$$\mathbf{M}_{ss} = (\mathbf{I} - \cos \theta e^{\mathbf{A}\text{TR}})^{-1} (e^{\mathbf{A}\text{TR}} - \mathbf{I}) \mathbf{A}^{-1} \mathbf{C}, \quad [26]$$

where \mathbf{I} is the $N \times N$ identity matrix. Defining

$$\mathbf{M}_0 = (M_{0S_1}, M_{0S_2}, \dots, M_{0S_N}) \quad [27]$$

and

$$\mathbf{M}_0 = \mathbf{I} \mathbf{M}_0, \quad [28]$$

the vector of saturation factors may be written

$$\mathbf{SF} \equiv \left(\frac{M_{\text{obs}S_1}}{M_{0S_1}}, \frac{M_{\text{obs}S_2}}{M_{0S_2}}, \dots, \frac{M_{\text{obs}S_N}}{M_{0S_N}} \right) = \mathbf{M}_0^{-1} \mathbf{M}_{ss} \sin \theta \quad [29]$$

and the magnetization actually experimentally observed is

$$\mathbf{M}_{\text{obs}} = \mathbf{M}_0 \mathbf{SF}. \quad [30]$$

The equations defining a system in chemical steady state as considered here take the form

$$\sum_{j \neq i} k_{S_iS_j} M_{0S_i} = \sum_{j \neq i} k_{S_jS_i} M_{0S_j} \quad [31]$$

for each species S_i . With the constraints imposed by Eq. [31], a direct calculation shows that

$$\mathbf{A} \mathbf{M}_0 = -\mathbf{C}, \quad [32]$$

so that

$$\mathbf{A}^{-1} \mathbf{C} = -\mathbf{M}_0. \quad [33]$$

Eq. [33] may be used to simplify Eqs. [26] and [29] under steady-state conditions, leading to an expression analogous to Eq. [1]:

$$\mathbf{SF} = \mathbf{M}_0^{-1} (\mathbf{I} - e^{\mathbf{A}\text{TR}} \cos \theta)^{-1} (\mathbf{I} - e^{\mathbf{A}\text{TR}}) \mathbf{M}_0 \sin \theta. \quad [34]$$

The fact that \mathbf{M}_0^{-1} does not commute through the rest of the expression to act on \mathbf{M}_0 results in the dependence of \mathbf{SF} on \mathbf{M}_0 .

SIMULATION RESULTS

Equation [34] for three exchanging species labeled A, B, and C was simulated in the Mathematica (Wolfram Research, Inc., Champaign, IL) programming language. Equation [31] as written for three species provides two independent constraints, so four of the six rate constants may be specified independently.

TABLE 1
Pseudo-Unimolecular Reaction Rate Constants for the Three Exchange Networks Discussed in the Text

	$k_{AB} = k_{BA}$	$k_{BC} = k_{CB}$	$k_{CA} = k_{AC}$
No exchange	0 s ⁻¹	0 s ⁻¹	0 s ⁻¹
Two site	1 s ⁻¹	0 s ⁻¹	0 s ⁻¹
Three site linear	1 s ⁻¹	1 s ⁻¹	0 s ⁻¹
Three site cyclic	1 s ⁻¹	1 s ⁻¹	1 s ⁻¹

Input parameters defining the pulse sequence and the underlying chemical characteristics of the system are

$$\{M_{0A}, M_{0B}, M_{0C}, T_{1A}, T_{1B}, T_{1C}, k_{AB}, k_{BA}, k_{AC}, k_{CA}; TR, \theta\}.$$

Values for these system input parameters were selected to illustrate the main results of the simulation without unnecessary complexity. In all cases we used $M_{0A} = M_{0B} = M_{0C} = 1$, and $T_{1A} = 5$, $T_{1B} = 3$, $T_{1C} = 1$. Values for the pseudo first-order reaction rates we used for each of the four possible exchange topologies are given in Table 1. Extensive numerical simulations confirm that the quantitative results to be described below are qualitatively similar to results obtained with other typical sets of input parameters.

Saturation Factors in the Presence of Chemical Exchange

Figure 2 shows the saturation factors of species A, B, and C under the four different exchange networks considered for a flip angle of 30°. Figure 3 shows the corresponding results for a flip angle of 90°. The SF's are clearly sensitive to the details of the exchange network and the pulse parameters, although many of the qualitative features of the behavior of SF's as a function of TR are independent of flip angle. For example, the curves all have a positive but decreasing slope across the full range of TR, and at both very short and very long TR the SF's approach values given by the Ernst formula, Eq. [1].

Saturation factors are not of independent interest but are used to derive T_1 's and concentrations. The errors that result from interpreting SF data in accordance with Eq. [1] are now demonstrated.

Apparent T_1 's in the Presence of Chemical Exchange

For the saturation factor SF_{S_i} of a species S_i , in chemical exchange, measured at a specific interpulse delay TR, Eq. [1] yields an apparent value for the spin-lattice relaxation time, T'_{1S_i} , of

$$T'_{1S_i} = \frac{-TR}{\ln\left(\frac{SF_{S_i} - \sin \theta}{SF_{S_i} \cos \theta - \sin \theta}\right)}. \quad [35]$$

SF_{S_i} and T'_{1S_i} depend on TR, θ , and all of the system's chemical parameters. In contrast, T_{1S_i} is an intrinsic property of species S_i . In general, $T'_{1S_i} = T_{1S_i}$ only if there is no chemical exchange involving species S_i . Figure 4 shows the departure of T'_1 from the true value of T_1 for the three species, A, B, and C, under the four different exchange networks considered, for a flip angle of 30°. Figure 5 shows the corresponding results for a flip angle of 90°.

It is clear that in the limit $TR \rightarrow 0$, the correct T_1 's are obtained; this will be discussed later more fully. However, when this condition is not satisfied, the measured values of the spin-lattice relaxation times are very different from the true system T_1 's. The degree of overestimate or underestimate depends upon the system parameters, but in general increases as TR increases. Figure 4 shows that a true value of $T_{1A} = 5$ s will be underestimated by nearly 3 s in the case of cyclic three-site exchange with the parameters as given. Comparable percentage errors occur for species B and C. The results shown for species B demonstrate that either overestimates or under-

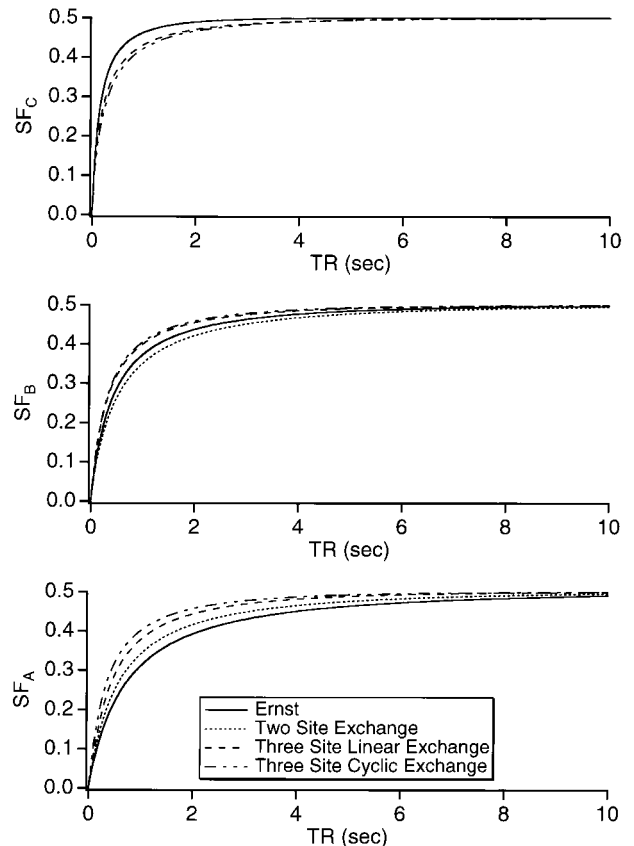


FIG. 2. Saturation factors for species A, B, and C under the four types of exchange networks possible in a three-site system, including that without exchange. Results are shown for a flip angle of 30°. Other parameters used in the simulation are $M_{0A} = M_{0B} = M_{0C} = 1$, $T_{1A} = 5$, $T_{1B} = 3$, $T_{1C} = 1$, and pseudo-unimolecular reaction rates as given in Table 1. Without loss of generality, the two-site network is defined as exchange between species A and B. Therefore the two-site exchange results and the nonexchanging (Ernst formula) results are identical for SF_C .

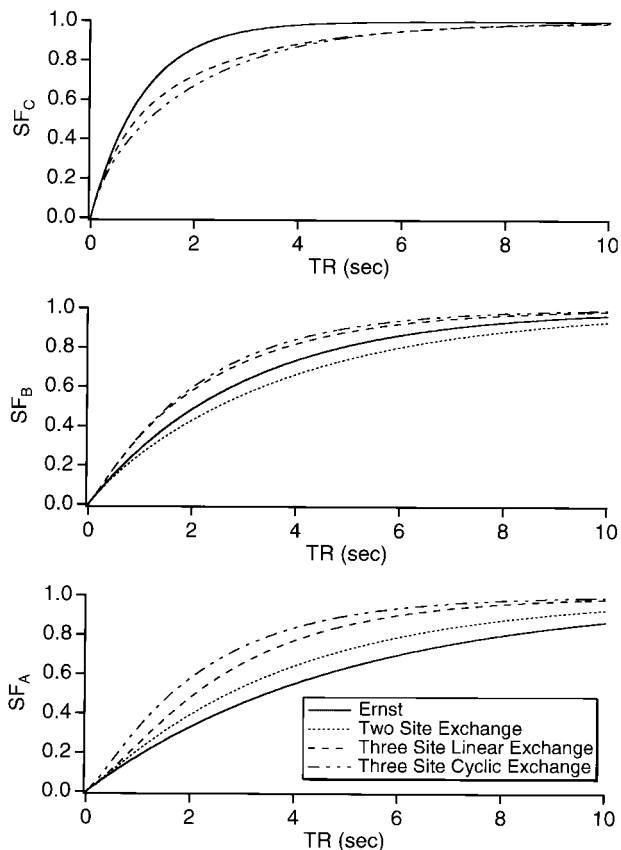


FIG. 3. Same as Fig. 2, only for a flip angle of 90° .

estimates of the spin–lattice relaxation time may occur, depending upon the system parameters. Comparing Figs. 4 and 5, it is clear that errors of comparable magnitude can occur for both flip angles. It is also evident that the TR must be made very small in both cases in order to ensure accuracy, although this restriction is somewhat less stringent with a larger flip angle. Nevertheless, even for that larger flip angle, a TR as short as, for example, 0.5 s, is still not sufficiently short to avoid significant error.

The strictness of the requirement for $TR \rightarrow 0$ to obtain accurate results depends upon the system parameters, including the nature of the exchange network. Table 2 shows the maximum TR that can be used to achieve T_1 measurements accurate to within 5 and 10% for $\theta = 90^\circ$. Results are presented for each of the three networks under consideration here. It is clear that the upper limit on TR depends on the particular resonance under consideration. The accuracy of all three T_1 's can be ensured by using the minimum of the appropriate three values of TR for a given set of parameters.

It is clear that the required upper bounds on TR are rather stringent. However, as indicated above, the strictness of the limit $TR \rightarrow 0$ can be somewhat relaxed by use of a larger flip angle. This is shown in Fig. 6, in which T_1' as a function of TR is shown for a wide range of flip angles for each of the three

species in a cyclic exchange network. Table 3 tabulates the data for specific error bounds. It is clear that even for $\theta = 90^\circ$, the requirements for short TR are very stringent. As θ approaches 150° , the minimum required TR exceeds 100 ms in all cases for 5% accuracy. This is possible to achieve in many *in vivo* systems, although it potentially requires the incorporation of homospoil pulses in the one-pulse sequence in order to avoid the effects of residual transverse magnetization (5).

An interesting feature of the asymptotic results for $TR \rightarrow \infty$ is shown in Fig. 7. For species which are connected by exchange processes, $T'_{1A} = T'_{1B} = T'_{1C}$ in the limit $TR \rightarrow \infty$. Comparable results for the two-site exchange network were shown in our previous studies (3–5). The rate at which the apparent spin–lattice relaxation times approach each other as a

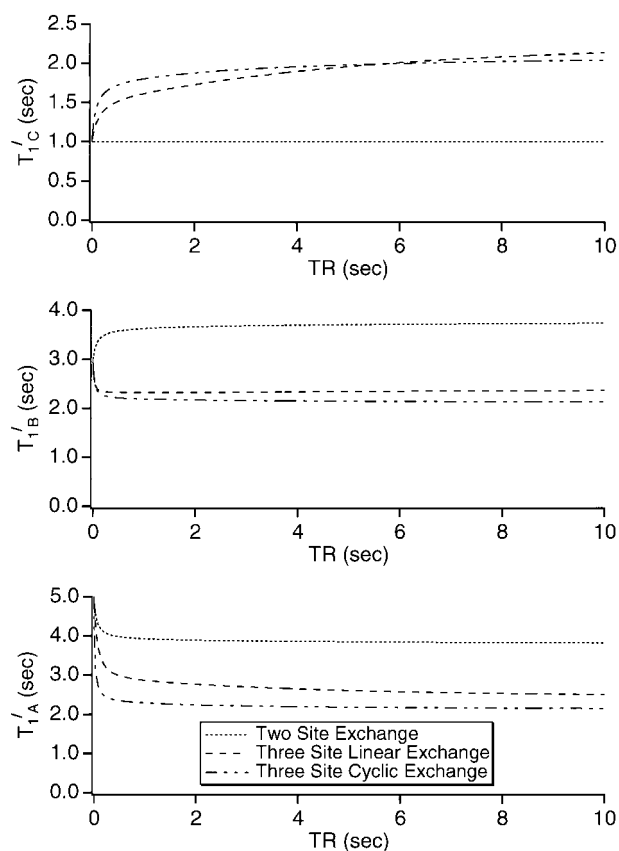


FIG. 4. Apparent spin–lattice relaxation times as a function of TR for species A, B, and C under the three types of networks with chemical exchange which are possible in a three-site system. T_1' is calculated from Eq. [35], neglecting the effects of chemical exchange. Results are shown for a flip angle of 30° . Other parameters used in the simulation are $M_{0A} = M_{0B} = M_{0C} = 1$, $T_{1A} = 5$, $T_{1B} = 3$, $T_{1C} = 1$, and pseudo-unimolecular reaction rates as given in Table 1. Results are not shown for the nonexchanging system, for which the Ernst formula, Eq. [1], is valid, since $T_1' = T_1$ for all TR and for each species in that case. The two-site network is defined as exchange between species A and B. Therefore, species C does not undergo exchange in that case, and $T'_{1C} = T_{1C}$ for all TR. It is clear that for all three species, $T_1' = T_1$ only in the limit $TR \rightarrow 0$. Otherwise, errors of 50% or more may occur. Deviations of T_1' from T_1 are indicative of the presence of chemical exchange.

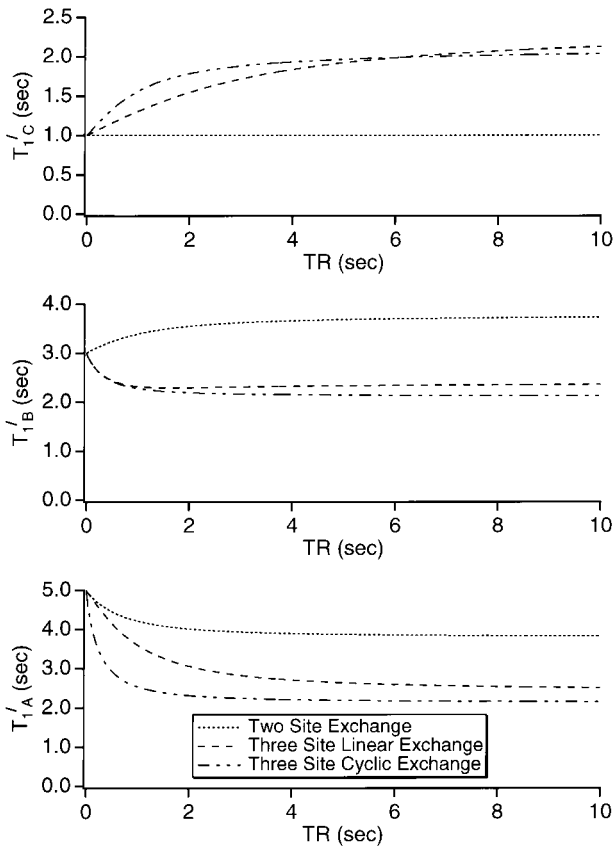


FIG. 5. Same as Fig. 4, only for a flip angle of 90° . By comparing Figs. 4 and 5, it is clear that significant departures from $T'_1 = T_1$ occur at somewhat larger values of TR for the larger flip angle.

function of TR depends upon the specific system parameters. In practical terms, the large TR limit is of little interest since the dynamic range of progressive saturation measurements decreases with increasing TR.

It should be noted that progressive saturation experiments designed to measure T_1 's typically use a sequence of several

TABLE 2
Upper Limits on TR for Accurate Measurement of T_{1A} , T_{1B} , and T_{1C} for the Three Exchange Networks Discussed in the Text

	TR _{max} (s) for T_{1A}	TR _{max} (s) for T_{1B}	TR _{max} (s) for T_{1C}	Relative error bound (%)
Two site	0.099	0.28	Any	5
	0.22	0.66	Any	10
Three site linear	0.086	0.072	0.15	5
	0.14	0.17	0.30	10
Three site cyclic	0.023	0.072	0.068	5
	0.050	0.17	0.13	10

Note. A flip angle of $\theta = 90^\circ$ is assumed throughout. For example, in order that the measurement of T_{1A} be accurate to within 5% in the two-site exchange network, $TR < 0.099$ s must be used.

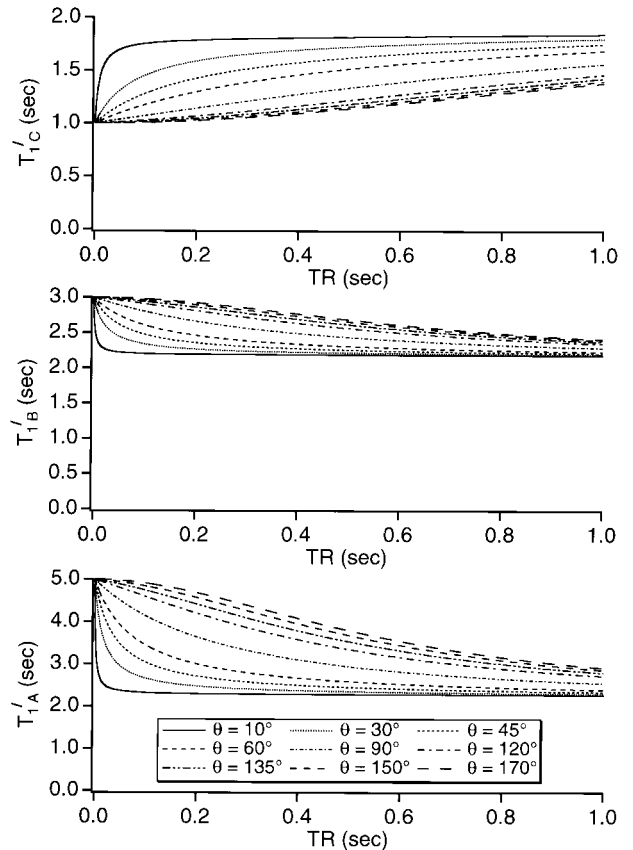


FIG. 6. Apparent spin-lattice relaxation times, T'_1 , as a function of TR for species A, B, and C undergoing three-site cyclic exchange. Results are shown for flip angles ranging between 10° and 170° . T'_1 is calculated from Eq. [35]. System parameters are $M_{0A} = M_{0B} = M_{0C} = 1$, $T_{1A} = 5$, $T_{1B} = 3$, $T_{1C} = 1$, and pseudo-unimolecular reaction rates as given in Table 1. It is clear that the apparent spin-lattice relaxation times equal the correct value only in the limit $TR \rightarrow 0$. For small flip angles, large errors occur even for extremely small TR. In fact, it is essentially impossible to perform accurate T_1 measurements when small flip angles are used. However, if large flip angles are used, accurate results may be obtained with values of TR which are more realistic.

TR's, $\{TR_i\}$, for which the data set $M_{\text{obs}}(\theta, TR_i)$ is fit to Eq. [1], rather than a comparison of equilibrium magnetization to observed magnetization for a single TR. This procedure does not address the fact that Eq. [1] is an incomplete description of the system. It can be shown numerically that this fitting procedure results in errors that are of the same order as those shown in Figs. 4 and 5.

SNR Consequences of Accuracy in T_1 Measurements

As discussed, it is a near-universal practice to pulse with $TR \approx T_1$ in order to increase the SNR per unit time. However, Fig. 6 and Table 3 show that only restricted choices of θ and TR result in accurate measurement of T_1 . Unfortunately, this results in a severe penalty in SNR. To show this, we make use of two results that follow readily from the Ernst and Anderson analysis of partial resonance saturation and from the general

TABLE 3

Upper Limits on TR for Accurate Measurement of T_{1A} , T_{1B} , and T_{1C} for the Three-Site Cyclic Exchange System Discussed in the Text

θ	TR _{max} (s) for T_{1A}	TR _{max} (s) for T_{1B}	TR _{max} (s) for T_{1C}	Relative error bound (%)
10°	0.0002	0.0005	0.0005	5
	0.0004	0.0015	0.0011	10
30°	0.0017	0.0054	0.0052	5
	0.0037	0.014	0.11	10
45°	0.0041	0.012	0.012	5
	0.0090	0.033	0.026	10
60°	0.0079	0.025	0.024	5
	0.018	0.064	0.050	10
90°	0.023	0.072	0.068	5
	0.050	0.17	0.13	10
120°	0.062	0.16	0.15	5
	0.12	0.32	0.26	10
135°	0.098	0.21	0.20	5
	0.18	0.39	0.32	10
150°	0.13	0.26	0.24	5
	0.22	0.44	0.37	10
170°	0.17	0.30	0.28	5
	0.26	0.48	0.41	10

Note. For example, in order that the measurement of T_{1A} be accurate to within 5% when a flip angle of $\theta = 10^\circ$ is used, a TR < 0.0002 s must be used.

definition of saturation factors. For a given observed SF and a fixed experimental time,

$$\text{SNR} \propto \text{SF}/\sqrt{\text{TR}}. \quad [36]$$

In addition, for a given TR, the flip angle θ_E at which maximum SNR is obtained for a resonance with spin–lattice relaxation time T_1 is given by

$$\cos \theta_E = e^{-\text{TR}/T_1}. \quad [37]$$

The flip angle defined by Eq. [37] maximizes SNR per unit time only for systems with negligible chemical exchange. However, because corresponding results incorporating chemical exchange are exceedingly complicated, we will use Eq. [37] as an estimate of the flip angle resulting in maximal SNR even for exchanging systems. The qualitative conclusions to follow will not be affected by this approximation. In general, Eq. [37] can only be satisfied for one component of a multiple-resonance spectrum, and many approaches to the problem of jointly optimizing the SNR of the various components are available. We will illustrate the results for the simple approach of using a flip angle $\theta_{E,\text{Avg}}$, that is, the average of the θ_E corresponding to each of the three resonances. Note that for T_1 measurements one typically would not use a set of parameters defined by Eq.

[37]. However, this parameter choice, which maximizes SNR, provides a convenient reference point for SNR comparisons.

Table 4 shows relative SNR for the three resonances for three choices of pulse parameters, as indicated. It is clear that the SNR is reduced by an order of magnitude for a selection of pulse parameters which permits accurate measurement of T_1 's. Thus, high SNR and accurate T_1 measurements using progressive saturation are mutually exclusive goals.

Apparent Resonance Amplitudes in the Presence of Chemical Exchange

The errors in measuring equilibrium magnetization ratios that result from the use of Eq. [1] for systems with complicated exchange networks will now be presented.

Assume that the value $M_A(\text{TR})$ is experimentally observed in a one-pulse experiment. Then the apparent equilibrium magnetization for species A, M'_{0A} , derived using Eq. [2] is

$$M'_{0A} = \frac{M_A(\text{TR})}{\text{SF}_A^{\text{Ernst}}(\text{TR})}, \quad [38]$$

where $\text{SF}_A^{\text{Ernst}}(\text{TR})$ denotes the SF derived for species A using the Ernst expression, Eq. [1]. In addition, by definition, the true equilibrium magnetization for species A, M_{0A} , satisfies

$$M_A(\text{TR}) = M_{0A}\text{SF}_A(\text{TR}). \quad [39]$$

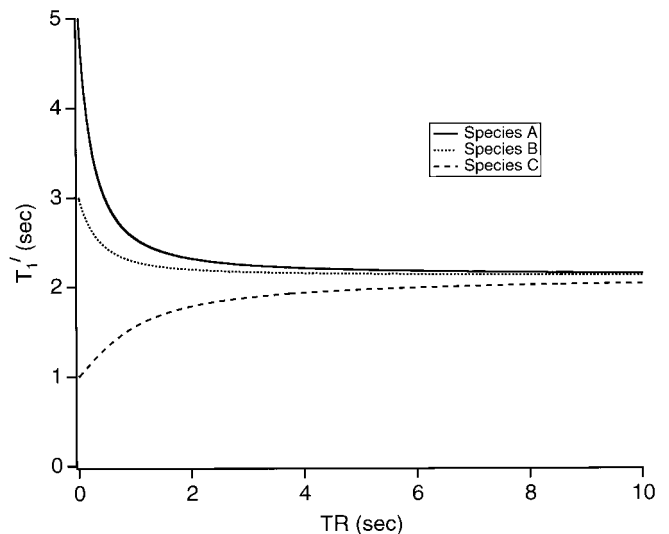


FIG. 7. Apparent spin–lattice relaxation times, T'_1 , as a function of TR for species A, B, and C undergoing three-site cyclic exchange. T'_1 is calculated from Eq. [35]. Results are shown for a flip angle of 90° , with system parameters $M_{0A} = M_{0B} = M_{0C} = 1$, $T_{1A} = 5$, $T_{1B} = 3$, $T_{1C} = 1$, and pseudo-unimolecular reaction rates as given in Table 1. This illustrates the fact that in the limit $\text{TR} \rightarrow \infty$, $T'_{1A} = T'_{1B} = T'_{1C}$.

TABLE 4
Signal-to-Noise Consequences of Selecting Parameters to Obtain Accurate Spin–Lattice Relaxation Times

	Parameter selection criteria		
	Error < 10% for all three T_1 's	TR = 1 s $\theta_{E,Avg}$ = average of Ernst angles	TR = 2 s $\theta_{E,Avg}$ = average of Ernst angles
Pulse parameters	$\theta = 150^\circ$ TR = 0.22 s	$\theta = 49^\circ$ TR = 1.0 s	$\theta = 63^\circ$ TR = 2.0 s
T'_{1A} (s)	4.51	2.35	2.28
T'_{1B} (s)	2.89	2.21	2.18
T'_{1C} (s)	1.04	1.73	1.83
Relative SNR(A)	1.0	16.48	16.33
Relative SNR(B)	1.0	10.85	10.65
Relative SNR(C)	1.0	4.40	4.15

Note. System parameters are as given in the text for the three-site system undergoing cyclic exchange. Column 1 pertains to a selection of TR ensuring that measured T_{1A} , T_{1B} , and T_{1C} are all within 10% of their true values when a flip angle of $\theta = 150^\circ$ is used. This choice of flip angle permits a reasonably long TR to be used. Column 2 shows results obtained with TR = 1 s and a flip angle which is the average of the Ernst angles for TR = 1 s for each species. Column 3 is similar to column 2, except with TR = 2 s. The apparent spin–lattice relaxation times, T'_{1A} , T'_{1B} , and T'_{1C} , as defined in the text, are the results of using Eq. [35] to calculate T_1 's from observed resonance saturation factors. Relative SNR(A) is the SNR obtained for resonance A, correctly accounting for chemical exchange effects, normalized to the value obtained using pulse parameters resulting in an error in T_1 of less than 10%. Relative SNR(B) and relative SNR(C) have similar meanings. It is clear that choosing TR and θ so that T_1 measurements are accurate to within 10% results in severe loss of SNR. For example, the SNR for resonance A is a factor of 16.48 greater when $\theta = 49^\circ$ and TR = 1.0 s are used than when $\theta = 150^\circ$ and TR = 0.22 s are used. However, the former choice leads to extremely inaccurate spin–lattice relaxation time measurements, while the latter choice ensures that the errors in these measurements due to chemical exchange effects will be less than 10%.

Therefore,

$$M'_{0A} = \frac{M_{0A} \text{SF}_A(\text{TR})}{\text{SF}_A^{\text{Ernst}}(\text{TR})}. \quad [40]$$

Equation [40] shows that the apparent corrected equilibrium magnetization for species A differs from its true value. Thus, the usual method of correcting magnetizations for partial saturation leads to manifestly incorrect results in systems with chemical exchange. Identical considerations hold for species B and C.

As was also the case for T_1 , we do not write out the explicit functional dependence of the M'_{0S_i} 's, but note here that they depend on all of the pulse and chemical parameters of the system. In general, $M'_{0S_i} = M_{0S_i}$ only if there is no chemical exchange involving species S_i .

Measurements of concentrations in NMR are frequently reported in terms of the ratio between two resonance ampli-

tudes, one of which may correspond to an external standard for quantification purposes. Therefore, for practicality, we will express further results in terms of resonance ratios. The TR dependence is indicated explicitly because we will plot results as a function of TR.

The apparent magnetization ratio of species A and B is given by

$$\frac{M'_{0A}}{M'_{0B}} = \frac{M_{0A}}{M_{0B}} \cdot \frac{\text{SF}_A(\text{TR})/\text{SF}_A^{\text{Ernst}}(\text{TR})}{\text{SF}_B(\text{TR})/\text{SF}_B^{\text{Ernst}}(\text{TR})}. \quad [41]$$

Similar expressions pertain to the ratio of any two species.

Figure 8 shows the departure of the apparent magnetization

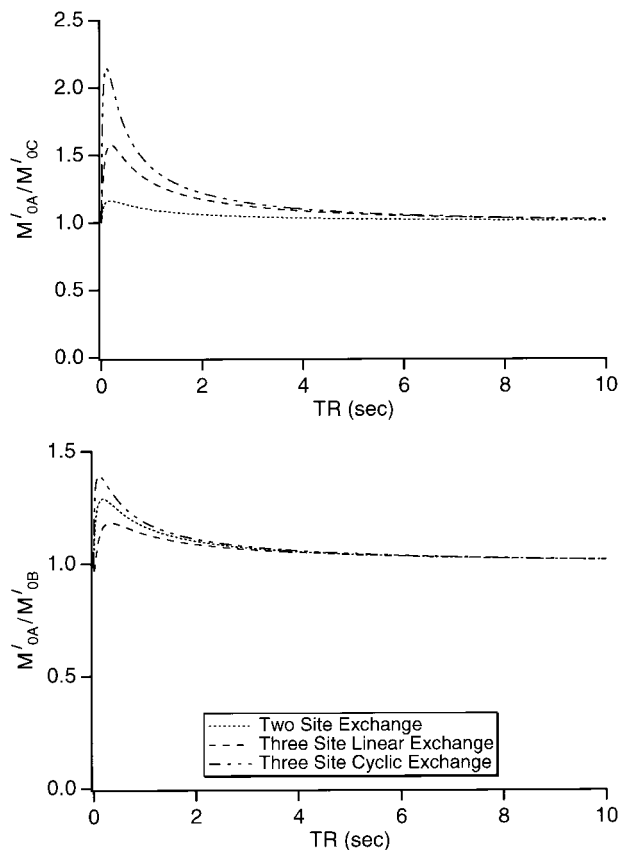


FIG. 8. Apparent magnetization ratios as a function of TR for species A, B, and C under the three types of chemical exchange networks that are possible in a three-site system. M'_{0A}/M'_{0C} and M'_{0A}/M'_{0B} , as defined in the text, are apparent magnetization ratios obtained by use of SF's derived from the Ernst formalism. Results are shown for a flip angle of 30° . Other parameters used in the simulation are $M_{0A} = M_{0B} = M_{0C} = 1$, $T_{1A} = 5$, $T_{1B} = 3$, $T_{1C} = 1$, and pseudo-unimolecular reaction rates as given in Table 1. With these parameters, the correct magnetization ratios are in all cases equal to unity. It is clear that for all three species, the apparent magnetization ratios equal the correct value only in the limits $\text{TR} \rightarrow 0$ and $\text{TR} \rightarrow \infty$. Otherwise, errors of 50% or more are seen to occur. Note that even though species C does not undergo chemical exchange in the two-site exchange network as defined here, ratios involving M_{0C} are still in error for general TR due to the effect of exchange on species A and B.

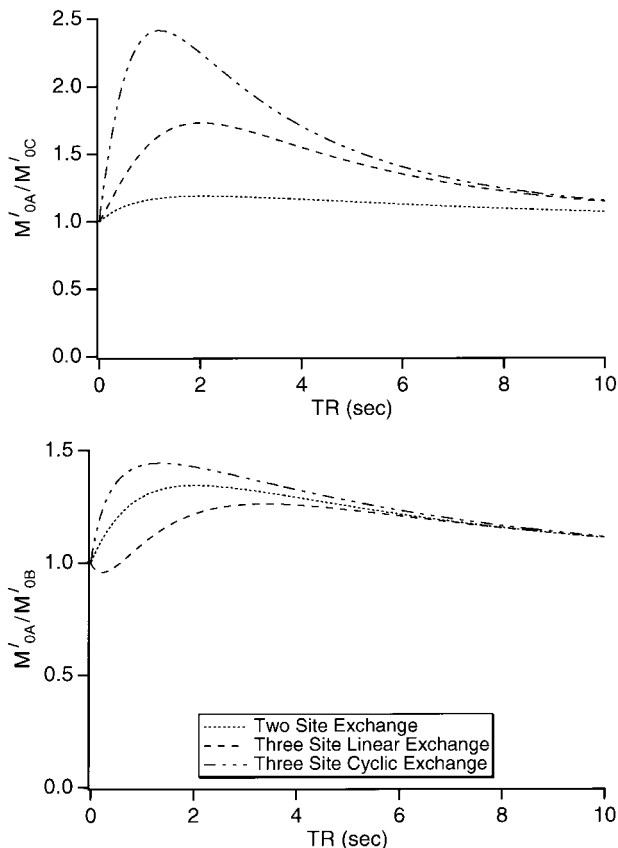


FIG. 9. Same as Fig. 8, but with a flip angle of 90° . By comparing Figs. 8 and 9, it is clear that the restriction on the maximum TR which leads to accurate measurements in the small TR regime is less stringent for larger θ . However, the apparent magnetization ratios converge to the correct values more rapidly for the smaller flip angle as $\text{TR} \rightarrow \infty$.

ratios, M'_{0A}/M'_{0B} and M'_{0A}/M'_{0C} , from the true values, $M_{0A}/M_{0B} = 1$ and $M_{0A}/M_{0C} = 1$, for the different exchange networks considered and a flip angle of 30° . Figure 9 shows the corresponding results for a flip angle of 90° . Again, it is clear that, while the sign and the magnitude of the errors depend upon the details of the system, the apparent magnetization ratios can be very different from the correct ratios for reasonable values of TR. It is readily seen that, unlike the case for T_1 measurements, not only the limit $\text{TR} \rightarrow 0$ but also the limit $\text{TR} \rightarrow \infty$ yields the correct ratios. For each of the two ratios and regardless of the exchange network, the accuracy of the measurement in the limit $\text{TR} \rightarrow 0$ is improved for larger θ , while in the limit $\text{TR} \rightarrow \infty$ it is improved for small θ .

Table 5 shows the maximum TR in the limit $\text{TR} \rightarrow 0$ that can be used to achieve magnetization ratio measurements accurate to within 5 and 10% for $\theta = 90^\circ$. Results are presented for each of the three exchange networks considered here. It is clear that the upper limit on TR depends on the particular ratio under consideration. The accuracy of both ratios can be ensured by using the minimum of the two appropriate values of TR for a given set of parameters. The results shown in Table 5

are representative; the strictness of the requirement for $\text{TR} \rightarrow 0$ depends upon all of the system parameters.

As noted in Figs. 8 and 9, the required upper bounds on TR for accurate ratio measurements in the regime $\text{TR} \rightarrow 0$ are just as stringent as for T_1 measurements, but can be relaxed by use of a larger flip angle. This is shown more explicitly in Fig. 10, in which the two independent magnetization ratios which are present in a three-component system are shown as a function of TR for a wide range of flip angles for the model three-site cyclic exchange network. Table 6 tabulates the data for specific error bounds. It is clear that for $\theta > 150^\circ$, the minimum required TR exceeds 100 ms for both ratios to achieve accuracy to within 5%. This TR is possible to achieve in most *in vivo* systems.

SNR Consequences of Accuracy in Resonance Amplitude Measurements

The tradeoff between accuracy and SNR can be examined in the same way as for the T_1 measurement case, as illustrated in Table 7. However, one important difference is that for amplitude measurements, both $\text{TR} \rightarrow 0$ and $\text{TR} \rightarrow \infty$ lead to accurate values. This latter limit is shown in the last column of Table 7. Note that according to Eq. [37], the optimal SNR for the $\text{TR} \rightarrow \infty$ limit is achieved with a flip angle of $\theta_E = 90^\circ$. Clearly, use of a long TR results in a superior combination of accuracy and SNR than does use of a short TR.

ANALYSIS OF THE N-SITE NETWORK

Explicit numerical results for $N > 3$ sites may be obtained in particular cases by a direct generalization of the methods outlined above, using either known chemical parameters or results based on reasonable guesses for the parameters. However, treatment of the general case provides useful results that apply to circumstances in which the number of exchanging sites, their relaxation times, concentrations, and reaction rates

TABLE 5
Upper Limits on TR for Accurate Measurement of the Ratios M_{0A}/M_{0C} and M_{0A}/M_{0B} for the Exchange Networks Discussed in the Text

	TR _{max} (s) for M_{0A}/M_{0C}	TR _{max} (s) for M_{0A}/M_{0B}	Relative error bound (%)
Two site	0.17	0.10	5
	0.40	0.21	10
Three site linear	0.074	0.83	5
	0.14	1.10	10
Three site cyclic	0.016	0.034	5
	0.033	0.075	10

Note. A flip angle of $\theta = 90^\circ$ is assumed throughout. For example, in order that the measurement of M_{0A}/M_{0C} be accurate to within 5% in the two-site exchange network, $\text{TR} < 0.17$ s must be used.

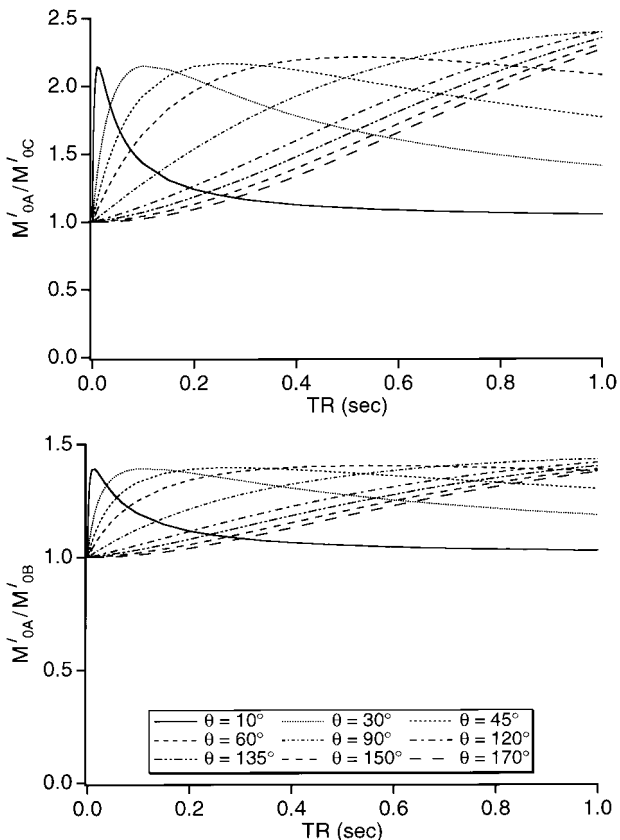


FIG. 10. Apparent magnetization ratios as a function of TR for species A, B, and C for the three-site cyclic exchange network. M'_{0A}/M'_{0C} and M'_{0A}/M'_{0B} , as defined in the text, are apparent magnetization ratios obtained by use of SF's derived from the Ernst formalism. Results are shown for flip angles ranging between 10 and 170°. Other parameters used in the simulation are $M_{0A} = M_{0B} = M_{0C} = 1$, $T_{1A} = 5$, $T_{1B} = 3$, $T_{1C} = 1$ and pseudo-unimolecular reaction rates as given in Table 1. It is clear that for all three species, the apparent ratios equal the correct value only in the limits $TR \rightarrow 0$ and $TR \rightarrow \infty$. In the small TR regime for small flip angles, large departures from the correct ratio occur even for extremely small TR. In fact, it is essentially impossible to perform accurate experiments in the small TR regime when small flip angles are used. If large flip angles are used, then accurate results may be obtained with longer values of TR in the small TR regime.

are not all known. Accordingly, we note some of the main properties of the general solution. We will make use of the fact that

$$\lim_{TR \rightarrow \infty} e^{\mathbf{A}TR} = \mathbf{0}, \quad [42]$$

where $\mathbf{0}$ is the $N \times N$ zero matrix.

This follows from the fact that all eigenvalues of \mathbf{A} are negative, by the Gerschgorin circle theorem (7).

Property 1. For a species S_i within any type of N -site exchange network,

$$\lim_{TR \rightarrow 0} SF_{S_i}(TR) = 0. \quad [43]$$

This result follows directly from Eq. [34]. Intuitively, it is accounted for by the fact that for rapid pulsing significant relaxation does not occur between pulses. The same limiting behavior occurs in the absence of chemical exchange.

Property 2. For a species S_i within any type of N -site exchange network,

$$\lim_{TR \rightarrow \infty} SF_{S_i}(TR) = \sin \theta. \quad [44]$$

This result follows directly from Eqs. [34] and [42], and is the same limiting behavior as in the case of no exchange. Intuitively, for long TR, complete longitudinal relaxation occurs to equilibrium; the approach to equilibrium, no matter how complex, does not affect the observations. According to Properties 1 and 2, in the limits $TR \rightarrow 0$ and $TR \rightarrow \infty$ chemical exchange does not change the values of saturation factors. This is illustrated for the three-site case in Figs. 2 and 3.

Property 3. If $T_{1S_1} = T_{1S_2} = \dots = T_{1S_N} \equiv T_1$, then

$$SF_{S_i}(TR) = \frac{(1 - e^{-TR/T_1}) \sin \theta}{(1 - e^{-TR/T_1} \cos \theta)} \quad [45]$$

for all species S_i and for all TR and θ .

Physically, this is because spin relaxation proceeds at the same rate regardless of which species in the exchange network a nucleus is located within. This can be proved by direct

TABLE 6
Upper Limits on TR for Accurate Measurement of the Ratios M_{0A}/M_{0C} and M_{0A}/M_{0B} for the Three-Site Cyclic Exchange Network Discussed in the Text

θ	TR _{max} (s) M_{0A}/M_{0C}	TR _{max} (s) M_{0A}/M_{0B}	Relative error bound (%)
10°	0.00012	0.00027	5
	0.00026	0.00060	10
30°	0.0011	0.0025	5
	0.0024	0.0057	10
45°	0.0028	0.0061	5
	0.0058	0.014	10
60°	0.0055	0.012	5
	0.010	0.026	10
90°	0.016	0.034	5
	0.033	0.075	10
120°	0.045	0.090	5
	0.085	0.17	10
135°	0.073	0.14	5
	0.13	0.24	10
150°	0.10	0.18	5
	0.16	0.29	10
170°	0.14	0.22	5
	0.20	0.33	10

Note. For example, in order that the measurement of M_{0A}/M_{0C} be accurate to within 5% when a flip angle of $\theta = 10^\circ$ is used, $TR < 0.00012$ s must be used.

TABLE 7
Signal-to-Noise Consequences of Selecting Parameters to Obtain Accurate Magnetization Ratio Measurements

	Parameter selection criteria			
	Error < 10% for M_{0A}/M_{0C} and M_{0A}/M_{0B}	TR = 1 s $\theta_{E,Avg}$ = average of Ernst angles	TR = 2 s $\theta_{E,Avg}$ = average of Ernst angles	TR = 5× longest T_1
Pulse parameters	$\theta = 150^\circ$ TR = 0.16 s	$\theta = 49^\circ$ TR = 1.0 s	$\theta = 63^\circ$ TR = 2.0 s	$\theta = 90^\circ$ TR = 25 s
M'_{0A}/M'_{0C}	1.09	1.86	1.14	1.01
M'_{0A}/M'_{0B}	1.04	1.33	1.79	1.01
Relative SNR(A)	1.0	20.07	19.89	8.76
Relative SNR(B)	1.0	12.90	12.66	5.48
Relative SNR(C)	1.0	5.05	4.76	1.93

Note. System parameters are as given in the text for the three-site system undergoing cyclic exchange. Column 1 pertains to a selection of TR ensuring that measured M_{0A}/M_{0C} and M_{0A}/M_{0B} are both within 10% of their true values when a flip angle of $\theta = 150^\circ$ is used. This choice of flip angle permits a reasonably long TR to be used. Column 2 shows results obtained with TR = 1 s and a flip angle which is the average of the Ernst angles for the three species for this TR. Column 3 is similar to column 2, except with TR = 2 s. Column 4 shows results for a very long TR and $\theta = 90^\circ$, which ensures correct ratio measurements. M'_{0A}/M'_{0C} and M'_{0A}/M'_{0B} are defined in the text as the apparent magnetization ratios, obtained by use of SF's derived from the Ernst formalism. Relative SNR(A) is the SNR obtained for resonance A using the formalism presented here, correctly incorporating chemical exchange, normalized to the value obtained using pulse parameters resulting in an error of <10%. Relative SNR(B) and relative SNR(C) have similar meanings. It is clear that choice of TR sufficiently small or sufficiently long that magnetization ratio measurements are accurate to within 10% results in severe loss of SNR. For example, the SNR for resonance A is a factor of 20.07 greater when $\theta = 49^\circ$ and TR = 1.0 s are used than when $\theta = 150^\circ$ and TR = 0.16 s are used. However, the former choice leads to extremely inaccurate ratio measurements, while the latter choice ensures that the errors in the measurements due to chemical exchange effects will be less than 10%. Use of a long TR with $\theta = 90^\circ$ permits accurate ratio measurements with less of a SNR per unit experimental time penalty than use of short TR.

calculation for the two-site case and confirmed by simulations for larger networks.

Property 4. If $T_{1S_1} = T_{1S_2} = \dots = T_{1S_N} \equiv T_1$, then

$$T'_{1S_i} = T_{1S_i} \quad [46]$$

for all species S_i and for all TR and θ .

This follows directly from Property 3 and Eq. [35].

Property 5. For a species S_i within any type of N -site exchange network,

$$\lim_{TR \rightarrow 0} T'_{1S_i} = T_{1S_i} \quad [47]$$

for any θ .

This follows after some calculation from Property 1 and the application of l'Hospital's rule to the explicit form of $T'_i(S_i)$ given by Eqs. [34] and [35]. Again, for rapid pulsing, significant chemical exchange does not occur between pulses; Eq. [1] is valid in that limit even with chemical exchange present. In practical terms this means that T_1 's can be determined by use of progressive saturation as long as the condition $TR \rightarrow 0$ is approached to a sufficient degree. The required limits on TR cannot be known with precision without a simulation based upon knowledge of the system's chemical parameters, which are the goal of the experiment and hence obviously unavailable in general. From the numerical results obtained for a represen-

tative case in the preceding section, it is clear that use of a large flip angle, on the order of 150° , may be required in order that the rapid pulsing condition is satisfied with values of TR sufficiently long to allow for data acquisition and the possible application of a homospoil pulse (see below).

Property 6. For N species $\{S_i\}$ within any type of exchange network,

$$\lim_{TR \rightarrow \infty} T'_{1S_1} = \lim_{TR \rightarrow \infty} T'_{1S_2} = \dots = \lim_{TR \rightarrow \infty} T'_{1S_N} \quad [48]$$

The limit is independent of θ , but depends upon the T_1 's. For a given exchange network, the limit is independent of the values of pseudo-unimolecular rate constants, assuming they are nonzero, although the rate of convergence to the limit does depend upon the rate constants. Of course if any rate constants are zero, the exchange network becomes qualitatively different and a different limiting value is obtained. The limit also depends upon equilibrium magnetizations, but if these magnetizations are varied in such a way that all of the M_{0S_i}/M_{0S_j} are unaltered, then the limit is unchanged.

This property has been resistant to direct proof but has been confirmed numerically for a wide range of exchange networks and chemical parameters.

Property 7. For a species S_i within any N -site exchange network, define $SF_{S_i}^{Einst}(TR)$, $SF_{S_i}(TR)$, and

$$M'_{0S_i} = \frac{M_{S_i}(\text{TR})}{\text{SF}_{S_i}^{\text{Ernst}}(\text{TR})} = \frac{M_{0S_i} \text{SF}_{S_i}(\text{TR})}{\text{SF}_{S_i}^{\text{Ernst}}(\text{TR})} \quad [49]$$

in analogy to Eqs. [38] and [40].

Then

$$\lim_{\text{TR} \rightarrow 0} M'_{0S_i}(\text{TR}) = M_{0S_i} \quad [50]$$

This follows from application of l'Hospital's rule to Eq. [49].

COROLLARY TO PROPERTY 7. For any two species S_i and S_j ,

$$\lim_{\text{TR} \rightarrow 0} \frac{M'_{0S_i}(\text{TR})}{M'_{0S_j}(\text{TR})} = \frac{M_{0S_i}}{M_{0S_j}} \quad [51]$$

This follows immediately from Property 7. The importance of this corollary is that quantification is typically performed through measurement of magnetization ratios. Thus, as stated earlier for the three-site case, it is true in general that concentration ratios calculated using the Ernst formula, Eq. [1], approach the actual ratios for short TR.

Property 8. With the same definitions as in the preceding property,

$$\lim_{\text{TR} \rightarrow \infty} M'_{0S_i}(\text{TR}) = M_{0S_i} \quad [52]$$

This follows immediately from Property 2. Note that one implication of this is that equilibrium magnetizations can in general be measured accurately by using a long TR and $\theta = 90^\circ$.

COROLLARY TO PROPERTY 8. For any two species S_i and S_j ,

$$\lim_{\text{TR} \rightarrow \infty} \frac{M'_{0S_i}(\text{TR})}{M'_{0S_j}(\text{TR})} = \frac{M_{0S_i}}{M_{0S_j}} \quad [53]$$

This follows immediately from Property 8 and shows that quantification of magnetization ratios may be accurately performed by the use of long TR experiments. Indeed, based on the numerical results shown in Table 7, there is a clear SNR advantage to implementing ratio measurements in the long TR limit rather than the short TR limit.

DISCUSSION

The pioneering paper by Ernst and Anderson in 1966 (1) formally analyzed the improvements in signal-to-noise that can result from the use of pulsed Fourier transform NMR rather than continuous-wave NMR. Part of the analysis treated what has come to be known as partial saturation of a resonance line

due to repetitive pulsing. The formalism developed in that paper was based on the Bloch equations for an isolated spin. The application of NMR spectroscopy to *in vivo* samples was still on the distant horizon, so that the need for incorporating chemical exchange into the analysis of the repetitive pulsing experiment by use of the Bloch-McConnell equations was not evident.

Subsequent to the publication of the Ernst and Anderson analysis of the one-pulse experiment, NMR spectroscopy has become an important tool for the analysis of *ex vivo* and *in vivo* physiologic systems. In all of this work (for references, see Ref. 5), partial saturation in a one-pulse experiment has been accounted for by use of Eqs. [1] and [2] in order to determine spin-lattice relaxation times and to obtain chemical concentrations. However, while exchange effects have been analyzed and accounted for in many of the experiments used in physiologic NMR studies, such as the various forms of saturation transfer (8-14) and inversion recovery (15, 16), the necessity for reanalyzing the ubiquitous one-pulse experiment to account for exchange was recognized only somewhat later (3).

Comparison of the Transient and Steady-State Analysis of Multiple-Site Exchange

A recent publication (17) provided an elegant description of the approach to equilibrium of an N -site exchanging system as described by Eq. [18]. It was found that the solution trajectory exhibited damped oscillations in the general case. In contrast, when detailed balance is satisfied, the approach to equilibrium could be described by a multiexponential approach to equilibrium magnetizations. While this description of the transient behavior of the spin system is of theoretical interest, it is rather limited in terms of applicability to the design and interpretation of actual NMR experiments. In contrast, in the present work we have examined the cyclic steady state of the N -site exchange network; it is precisely this steady state which is actually observed in virtually all one-pulse experiments on *in vivo* systems or other systems exhibiting exchange.

Problems Arising in Short TR Experiments

The significance of the results described herein for specific applications depends entirely upon the extent to which the addition of chemical exchange to the formalism affects the actual calculated values of spin-lattice relaxation times and magnetizations. In previous work (3-5) we showed theoretically and in both *in vitro* and in *in vivo* experiments that the errors that result from neglecting exchange in typical systems can be very large. An important corollary for practical applications was the demonstration that the Ernst formula, Eq. [1], remains valid for exchanging systems when the interpulse delay time is sufficiently small. Hence, under rapid pulsing conditions, estimates of spin-lattice relaxation times and corrections for partial saturation based on Eqs. [1] and [2] may be correctly obtained.

The minimum TR which can be used is constrained by the data acquisition period and therefore by the spectral resolution required. A further practical difficulty is that when the fast pulsing condition is satisfied, one typically has $TR \approx T_2$. This leads to transverse magnetization interference effects that are neglected in Eq. [1]. While these effects may be incorporated by an appropriate reformulation of the problem, it is much simpler in practice to modify the one-pulse sequence so that a homospoil pulse is placed after each signal acquisition period (4, 5). Note that the time required to execute this homospoil pulse will place a further constraint on the minimum practicable TR.

Significance of the Extension of the Formalism from Two Sites to Three and N Sites

A serious limitation of our previous analysis of the one-pulse experiment in the presence of chemical exchange was that the formalism only accounted for exchange between two sites. However, metabolites in typical physiologic systems may simultaneously participate in three or more reactions. Accordingly, a full treatment of the three-site mutual exchange was undertaken in the present paper. A more general mathematical approach was taken than in our earlier work (3), permitting the results to be expressed compactly for arbitrarily complex (N -site) exchange networks. The simulation results clearly demonstrate the fact that the addition of a third site can markedly change estimates of T_1 's and chemical concentrations.

Application of the N-Site Analysis to the Empirical Determination of Saturation Factors

Corrections of apparent equilibrium magnetizations for partial saturation are most often carried out without explicit knowledge of T_1 's. At a given experimental period (Period 1, say), nonsaturated magnetization is measured in a one-pulse experiment by use of a long TR. A short TR experiment is then performed immediately with the same θ , still during Period 1, and the SF is calculated based on the results of these two measurements in accordance with Eq. [2]. At a subsequent time (during Period 2, say), e.g., after an intervention such as altering substrate availability or changing temperature, further data are obtained with the short value of TR, since this results in greater SNR per unit time than if a long TR is used. The SF determined during Period 1 is then used to correct the data obtained during Period 2 for partial saturation. An implicit but generally reasonable assumption in this procedure is that the T_1 's do not change throughout the course of the experiment. It is important to note, however, that the results presented here show that such a correction scheme is entirely invalid in the presence of chemical exchange and may lead to large errors unless all of the system's M_0 's and k 's, in addition to the T_1 's are unchanged. That is, this naive but universally applied correction scheme is valid only when nothing happens to the sample.

Application of the N-Site Analysis to the Determination of Spin-Lattice Relaxation Times

As noted above, the typical progressive saturation experiment involves measurement of SF(TR_i) for a set of predetermined TR_i 's with constant θ and then fitting the results to Eq. [1] to determine T_1 . However, we have demonstrated that the SF's are not merely functions of TR and θ , but rather of all parameters describing the chemical system. It is clearly not realistic to attempt to fit the progressive saturation data to the full analytic form of the results; the signal-to-noise ratio required for such a multiparameter fit to be meaningful simply cannot be obtained. This issue was specifically addressed in earlier work (4) for the case of two-site exchange, in which a result corresponding to Property 5 of the present work was described. Here, we have extended this to the N -site case and found that, regardless of the exchange network involved, rapid pulsing with a suitably large flip angle permits the Ernst formula to be correctly applied to one-pulse data. Thus, T_1 's can still be obtained rigorously in a relatively simple fashion, but only if rapid pulsing and a large flip angle are used, with the constraints on TR and θ being set with reference to simulation results comparable to those presented in Table 3.

Relaxing the short TR constraint leads to the dependence of T_1' , as defined in Eq. [35], on TR. In fact, this dependence may be taken as the signature of a species which is undergoing a significant amount of exchange. This was previously demonstrated experimentally using ^{31}P NMR spectroscopy of the rat gastrocnemius muscle (5). Variation of T_1' as a function of TR was found for the phosphorus nucleus of phosphocreatine and for $[\gamma\text{-}^{31}\text{P}]\text{ATP}$, which are undergoing rapid exchange via the creatine kinase reaction, but not for $[\alpha\text{-}^{31}\text{P}]\text{ATP}$, which undergoes only minimal exchange in this system.

Application of the N-Site Analysis to the Determination of Magnetizations

As shown here, there are two ways to obtain the correct equilibrium magnetizations. First, a procedure making use of rapid pulsing may be employed, as was also the case for T_1 determinations. A long TR experiment followed by an experiment with suitably short TR and large θ , based on estimates for the chemical parameters of the system under investigation, are performed during Period 1. To ensure that TR is sufficiently small and that θ is sufficiently large, reference must be made to simulation results comparable to those presented in Table 6. The ratio of the observed magnetizations, that is, the saturation factor, is then given by Eq. [1]; in particular, the saturation factor is independent of any of the system M_0 's and k 's. During Period 2, data are taken with the same short TR and large θ and corrected for rapid pulsing using the previously determined saturation factor in accordance with Property 7. An alternative procedure makes use of Property 8; TR must be sufficiently long that essentially full relaxation to equilibrium occurs between pulses. Using this approach, there is no need to

explicitly measure saturation factors. Of course, the suboptimal SNR resulting from this time-consuming process is precisely what one wishes to avoid by the usual method of pulsing fairly rapidly and then using saturation factors to correct for partial saturation of resonances. Unfortunately, however, to avoid systematic errors associated with chemical exchange, long TR experiments or else extremely short TR experiments are now seen to be a requirement. While the SNR ratio which results is severely degraded (cf., Table 7) in either case, it appears that the penalty is significantly less for long TR experiments.

Dependence of Apparent Spin–Lattice Relaxation Times and Magnetizations on System Parameters

Our previous general analysis of the two-site exchanging system (3) also presented simulation results for saturation factors and errors in magnetization ratios due to assuming the validity of the Ernst relation, Eq. [1]. Results were displayed as a function of reaction rate, showing that departures from results based on the Ernst and Anderson analysis were, as expected, greater for larger exchange rates. In addition, errors in magnetization ratios were presented as an explicit function of changing chemical concentrations, since saturation factors in the presence of chemical exchange are strongly dependent upon equilibrium magnetizations. In the present work we have emphasized the dependence of saturation factors, apparent spin–lattice relaxation times, and magnetization ratios on TR and θ , since those are the most readily varied experimental parameters. However, it can be shown that results may be obtained for the three-site case which are fully analogous to those in the previous analysis of the two-site case with respect to variation of reaction rates and concentrations as independent variables.

In experiments such as inversion transfer and inversion recovery, an effective T_1 , $T_{1,\text{eff}}$, is often defined by

$$\frac{1}{T_{1,\text{eff}}} = \frac{1}{T_1} + k, \quad [54]$$

where k is the pseudo-unimolecular reaction rate for reactions contributing to the chemical–kinetic decay of the species in question. Obviously, changes in $T_{1,\text{eff}}$ may be due to changes in either T_1 or in k , and the experiment in general cannot distinguish between these possibilities without additional experimental data. Nevertheless, it is occasionally useful to monitor $T_{1,\text{eff}}$ to examine, for example, the effect of an intervention. In that case, it is often a reasonable assumption that T_1 is largely unchanged. Results may then be interpreted in terms of changes in reaction rates. In contrast, in the one-pulse experiment analyzed in the present work, it is essentially impossible to define a physically meaningful effective T_1 that incorporates exchange effects. Not only is there no simple formula for an effective T_1 in the one-pulse experiment, but in addition the effective T_1 depends on all M_0 's, T_1 's, and k 's for the exchanging system. Thus, changes in the effective T_1 are in general

uninterpretable in simple terms. Such changes may be due to changes in true spin–lattice relaxation times or M_0 's of any species in the exchange network or to changes in reaction rates.

Applicability of the Formalism to NMR Imaging Experiments

Finally, we note that the above considerations are also relevant to MRI data analysis. An expression related to Eq. [1],

$$M_{\text{obs}}(\text{TR}, \text{TE}) = C \cdot (1 - e^{-\text{TR}/T_1}) \cdot e^{-\text{TE}/T_2}, \quad [55]$$

appears frequently in the MRI literature as a description of image intensity in spin-echo imaging. Here, TR is the time interval between successive applications of an imaging sequence, TE is a spin-echo time, $M_{\text{obs}}(\text{TR}, \text{TE})$ is the observed magnetization in an imaging pixel, and C is a constant of proportionality which may also include effects such as diffusion. This expression may be used to determine the T_1 of mobile water, for example, on a pixel-by-pixel basis by fixing TE and varying TR in a series of experiments. However, the water protons within an imaging pixel may in general undergo chemical exchange with water protons within a pool with a different T_1 . This may be due to exchange with neighboring tissue types or to exchange with relatively immobile water. It is clear from the considerations detailed above that, under these conditions, the values of tissue T_1 's derived from use of Eq. [55] may be highly inaccurate. Similar considerations hold for other imaging sequences.

CONCLUSIONS

The one-pulse sequence is the most commonly performed NMR experiment. The Ernst formula, Eq. [1], is often used to derive values for T_1 's. Similarly, a correction based on Eq. [1] or an empiric correction based on observed SF's is often used to derive chemical or metabolite concentrations from one-pulse experiments. However, both the Ernst formula and this empiric correction scheme based on observed SF's are valid only for nonexchanging systems. When applied to samples undergoing chemical exchange, including most physiologic systems, these methods yield results that are highly inaccurate. In this work, new expressions have been derived which explicitly account for chemical exchange in a system with an arbitrary N -site exchange network undergoing repetitive pulsing. To obtain reliable T_1 's very short TR's must be used in conjunction with large flip angles. To obtain reliable concentration measurements, either very short TR's must be used in conjunction with large flip angles or else long TR's must be used. For both types of measurements, the goals of achieving high SNR and of avoiding large systematic errors due to chemical exchange effects are, in general, mutually inconsistent.

ACKNOWLEDGMENTS

The authors thank George Weiss for his suggestion of the use of the Gerschgorin circle theorem and Alena Horská for useful discussions.

REFERENCES

1. R. R. Ernst and W. A. Anderson, Application of Fourier transform spectroscopy to magnetic resonance. *Rev. Sci. Instrum.* **37**, 93–102 (1966).
2. R. Freeman and H. D. W. Hill, Fourier transform study of NMR spin–lattice relaxation by “progressive saturation.” *J. Chem. Phys.* **54**, 3367–3377 (1971).
3. R. G. S. Spencer, J. A. Ferretti, and G. H. Weiss, NMR saturation factors in the presence of chemical exchange. *J. Magn. Reson.* **84**, 223–235 (1989).
4. A. Horská, J. Horský, and R. G. S. Spencer, Measurement of spin–lattice relaxation times in systems undergoing chemical exchange. *J. Magn. Reson. A* **110**, 82–89 (1994).
5. A. Horská and R. G. S. Spencer, Measurement of spin–lattice relaxation times and kinetic rate constants in rat muscle using progressive partial saturation and steady-state saturation transfer. *Magn. Reson. Med.* **26**, 232–240 (1996).
6. H. M. McConnell, Reaction rates by nuclear magnetic resonance. *J. Chem. Phys.* **28**, 430–431 (1958).
7. G. Strang, “Introduction to Applied Mathematics,” Wellesley–Cambridge Press, Wellesley, MA (1986).
8. S. Forsén and R. A. Hoffman, A new method for the study of moderately rapid chemical exchange rates employing nuclear magnetic double resonance. *Acta Chem. Scand.* **17**, 1787–1788 (1963).
9. S. Forsén and R. A. Hoffman, Study of moderately rapid chemical exchange reactions by means of nuclear magnetic double resonance. *J. Chem. Phys.* **39**, 2892–2901 (1963).
10. S. Forsén and R. A. Hoffman, Exchange rates by nuclear magnetic multiple resonance. III. Exchange reactions in systems with several nonequivalent sites. *J. Chem. Phys.* **40**, 1189–1196 (1964).
11. R. A. Hoffman and S. Forsén, Transient and steady-state Overhauser experiments in the investigation of relaxation processes, analogies between chemical exchange and relaxation. *J. Chem. Phys.* **45**, 2049–2060 (1966).
12. J. A. Bittl and J. S. Ingwall, Reaction rates of creatine kinase and ATP synthesis in the isolated rat heart. *J. Biol. Chem.* **260**, 3512–3517 (1985).
13. K. Ugurbil, Magnetization-transfer measurements of individual rate constants in the presence of multiple reactions. *J. Magn. Reson.* **64**, 207–219 (1985).
14. R. G. S. Spencer, J. A. Balschi, J. S. Leigh, and J. S. Ingwall, ATP synthesis and degradation rates in the perfused rat heart. ³¹P-Nuclear magnetic resonance double saturation transfer measurements. *Biophys. J.* **55**, 921–929 (1988).
15. R. A. Meyer, M. J. Kushmerick, and T. R. Brown, Application of ³¹P NMR spectroscopy to the study of striated muscle metabolism. *Am. J. Physiol.* **242**, C1–C11 (1982).
16. H. Degani, M. Laughlin, S. Campbell, and R. G. Shulman, Kinetics of creatine kinase in heart: A ³¹P NMR saturation- and inversion-transfer study. *Biochemistry* **24**, 5510–5516 (1985).
17. J. C. McGowan, J. Schotland, and J. S. Leigh, Oscillations, stability, and equilibrium in magnetic exchange networks. *J. Magn. Reson. A* **108**, 201–205 (1994).